Research Article

Spatio-Temporal Variations of Land-Use Land-Cover in Response to RUSLE Model in Swat Basin Using Remote Sensing and GIS Techniques

Sumaira Kousar* and Safdar Ali Shirazi

Institute of Geography, University of the Punjab, Lahore, Pakistan.

Abstract | Soil erosion stands as a formidable challenge, particularly in regions susceptible to a confluence of natural and anthropogenic factors. This study endeavors to unravel the intricacies of soil erosion within the Swat district, employing the Revised Universal Soil Loss Equation (RUSLE) model alongside cutting-edge Remote Sensing (RS) and Geographic Information System (GIS) techniques. The RUSLE model, celebrated for its simplicity and efficiency, offers a lens to assess soil losses quantitatively, categorizing the basin area into five distinct vulnerability groups predicated on their proneness to soil erosion. The study's findings spotlight alarming terrain vulnerability, specifically in the district's northern expanse, encompassing locales like Kalam, Bahrain, and Pashmal. Within these regions, the magnitude of exposure is underscored by an average soil loss of 31.25 tonnes per hectare per year, coupled with compelling evidence of substantial erosion. The specter of erosion's far-reaching implications beckons for immediate intervention, especially for the 2% of land grappling with extreme soil erosion. Urgent measures are imperative to preserve land integrity and safeguard the communities reliant on these resources. The amalgamation of GIS with the RUSLE model is indispensable in grappling with soil erosion's complex tapestry. This synergy empowers soil conservation agencies to channel resources toward high-vulnerability regions, sculpting a landscape of proactive land preservation. As the study concludes, the imperative for future research echoes louder, beckoning to decipher the intricate web of contributors to soil erosion. The tale of soil preservation is far from over; it transforms into a symphony of knowledge and action orchestrated to better our shared terrestrial environment.

Received | August 16, 2023; **Accepted** | September 11, 2023; **Published** | September 20, 2023
***Correspondence** | Sumaira Kousar, Institute of Geography, University of the Punjab, Lahore, Pakistan; **Email:** sumaira.geog@gmail.com
Citation | Kousar, S. and S.A. Shirazi. 2023. Spatio-temporal variations of land-use land-cover in response to RUSLE Model in Swat basin using remote sensing and GIS techniques. *Sarhad Journal of Agriculture,* 39(3): 722-737.
DOI | https://dx.doi.org/10.17582/journal.sja/2023/39.3.722.737
Keywords | Soil erosion, Spatial assessment, RUSLE, Remote sensing, GIS, Swat, Pakistan

Introduction

The health of the soil is inherently crucial in meeting essential human requirements, such as sustenance, textiles, uncontaminated water, and unpolluted air, within the twenty-first century framework (Amundson *et al.*, 2015). Soil plays a crucial role in effectively operating Earth's systems, enabling the supply of vital functions within ecosystems (Robinson *et al.*, 2017; Keesstra *et al.*,

2016). Nevertheless, the acts of humans and the pressures exerted by the environment can diminish soil quality (Borrelli *et al.*, 2017). Soil erosion is a significant issue, with key factors being population growth, deforestation, and overgrazing (Emadodin and Bork, 2012). The ramifications of erosion are diverse and have substantial importance for many reasons. The initial process of soil erosion, which involves the removal of the uppermost layer of soil known as topsoil, substantially impacts soil fertility and agricultural productivity. Secondly, erosion results in a decline in reservoirs overall capacity and functionality, while simultaneously deteriorating the downstream water quality (El-Jazouli *et al.*, 2017; Gayen and Saha, 2017). In addition, the consequences of soil erosion have implications in various other aspects.

Moreover, soil erosion increases pollutants and sediment deposition in streams and rivers, ultimately leading to the obstruction of these aquatic systems and a reduction in biodiversity (Allafta and Opp, 2022). In addition, erosion contributes to the downstream transportation of water containing silt, leading to sediment layers that impede the natural flow of streams and rivers. Consequently, this phenomenon contributes to the incidence of floods (Gayen and Saha, 2017). Soil erosion has a significant role in reducing land resources that would otherwise facilitate the growth of flora, which possesses the capacity to absorb carbon dioxide, a greenhouse gas associated with climate warming. Notably, soils can sequester a considerable quantity of greenhouse gases, potentially mitigating around five percent of anthropogenic greenhouse gas emissions during a specific timeframe (Allafta and Opp, 2022). An alarming number reveals that an estimated 10 million hectares of croplands experience significant degradation annually as a result of the persistent effects of soil erosion.

Overpopulation exacerbates problems such as deforestation for agriculture and the extraction of wood and other resources, intensifying their negative impacts (Kheir *et al.*, 2008; Nekhay *et al.*, 2009; Tongde *et al.*, 2021). Regrettably, human activities bear primary responsibility for soil degradation, which has emerged as a critical issue in recent times (Wiejaczka *et al.*, 2017). These activities affect every aspect of land use and can be further compounded by natural factors such as landscape and climate changes (Kriegler *et al.*, 2013). The conversion of natural vegetation is the most apparent consequence of these activities, leading to multiple ecological implications (Bucała *et al.*, 2015). The shift from natural vegetation to agriculture has aggravated the problem, especially in hilly regions. Intensive agricultural practices have significantly increased soil erosion rates due to this land use change, posing grave threats to the environment and the economy (Nearing *et al.*, 2017).

The global ramifications of land erosion are profound, exerting a significant impact on critical domains including agricultural output, water infrastructure, and recreational spaces. This translates into a substantial annual economic burden, estimated at approximately $7 billion on a global scale (Borrelli *et al.*, 2020; Hewett *et al.*, 2018). The implications extend deeply into crucial sectors like agriculture, water storage facilities, and leisure areas, intensifying the threat of floods and infrastructure impairment due to the accumulation of sediments (FAO, 2011; Wuepper *et al.*, 2020; Yang *et al.*, 2003; Alewell *et al.*, 2020). Throughout the previous century, the escalation of land degradation has led to a staggering loss of topsoil productivity, amounting to 24 million tons globally (Ullah *et al.*, 2022). Alarming forecasts by the UN Food and Agriculture Organization indicate that 90% of the world's topsoil could be endangered by 2050, underlining the pressing imperative for adopting sustainable land management practices (FAO, 2019). Insights from studies reveal that reservoirs worldwide encounter an annual decline in storage capacity, ranging from 0.5% to 1% due to sedimentation. Disturbingly, projections indicate that by the 2050s, numerous dams might be left with only half their current storage capacity, reinforcing the urgency of addressing this issue (Chuenchum *et al.*, 2020).

Annually, an unsettling reality unfolds as the reservoirs worldwide experience a gradual decline in their storage capacity due to sedimentation, ranging between 0.5% and 1%, as highlighted in the study conducted by Chuenchum and colleagues (Chuenchum *et al.*, 2020). This sobering observation is compounded by the projection that many dams could be left with merely half of their existing capacity by the 2050s. Particularly disconcerting trends emerge in Asia, where reservoir storage capacity is being eroded by sedimentation at an alarming rate, consuming up to 40% of the capacity, posing a substantial hazard to future water supply reliability, as indicated by (Walling, 2011).

Vulnerable to the scourge of soil erosion, developing nations face heightened risks. This reality is starkly evident in India, where water erosion affects a vast expanse of land approximately 30-32.8 million hectares as underscored by (Lal, 2017). In Iran, recent investigations by (Mohammadi *et al*., 2018) divulge that the country grapples with a worrisome average annual soil loss of 24 tons per acre. Similarly, Pakistan contends with the profound impact of water erosion, resulting in soil loss across over 11.2 million hectares, encompassing nearly 70% of the country's total land area, as elucidated by (Ashraf *et al*., 2017).

For more than seven decades, the adoption and application of soil erosion models have played a pivotal role in both predicting and mitigating soil erosion. This field has seen the establishment of various influential models, each contributing to our understanding of this critical phenomenon. Some notable models include the Water Erosion Prediction Project (WEPP) (Boardman, 2006; Choudhury *et al*., 2022), the Soil and Water Assessment Tool (SWAT) (Boardman, 2006), the Revised Morgan and Finney model (RMMF) (Morgan, 2001), the Soil Erosion Model for Mediterranean Regions (SEMMED) (Boardman, 2006), and the European Soil Erosion Model (EUROSEM) (Boardman, 2006). Among these models, the Universal Soil Loss Equation (USLE) stands out as an extensively utilized empirical model for estimating soil erosion. It presents a moderate level of complexity in contrast to other models (Ganasri and Ramesh, 2016). Over the course of the past eight decades, researchers have consistently turned to the RUSLE model for its exceptional attributes, including high accuracy, flexibility, reliability, simplicity, and user-friendliness (Meliho *et al*., 2020; Boardman *et al*., 2009; Sandeep *et al*., 2021; Aslam *et al*., 2020).

The fundamental aim of this study is to quantify the extent of soil erosion within the Swat district by establishing a comprehensive overview of soil loss dynamics. This objective will be realized through the integration of Remote Sensing (RS) data and Geographic Information System (GIS) techniques in conjunction with the Revised Universal Soil Loss Equation (RUSLE) model. This integration will facilitate the creation of maps that delineate the varying degrees of erosion severity across different regions within the Swat district and identify the contributing factors. These generated maps will offer a tangible visualization of erosion patterns, enhancing our understanding of the phenomenon.

Materials and Methods

Study area

The Swat district is positioned in Khyber Pakhtunkhwa, Pakistan, at coordinates 34˚46'58" N and 72˚21'43" E. The district shares its northern boundary with Chitral, the western border with Dir, and the northeastern border with Gilgit-Baltistan. Encompassing an expanse of 5,337 square kilometers, the district is inhabited by approximately 1.26 million individuals (Bangash, 2012). Nestled within the heart of Khyber Pakhtunkhwa's thriving tourist industry, the study area is distinguished by its mountainous topography, encircled by the majestic Hindu Kush Himalayas (Qasim *et al*., 2013). The climate within Swat exhibits a diverse range, spanning from semiarid to subhumid to humid, thereby showcasing a spectrum of climatic conditions (Zamani *et al*., 2022). From a geological perspective, the research area resides within a Suture Zone (SZ), formed as a result of the convergence between the Indian Plate and the Kohistan Island Arc (KIA). This region marks a particularly active tectonic and geomorphic zone, where the KIA interfaces with the Asian Plate (Islam *et al*., 2022). The annual precipitation in this region fluctuates between 600 to 1200 mm (Dahri *et al*., 2011; Bazzani, 2013). To sustain their livelihoods, the local populace heavily relies on the area's natural resources, including farmland, pastures, livestock, fisheries, tourism sites, and timber (Khan and Khan, 2009). Agriculture is significant in the district's economy, with approximately 42% of the population deriving their income from it (Bacha *et al*., 2021). For enhanced clarity, Figure 1 visually situates the study area within Pakistan, providing a clear overview of its geographical context. In addition, Figure 2 offers a digital elevation model and slope analysis, offering insights into the topographical features of the research region.

RUSLE model

The Universal Soil Loss Equation (USLE) stands as a widely adopted model for comprehending the intricate dynamics of soil erosion. Within this study, the Revised Universal Soil Loss Equation (RUSLE) was employed, harnessing actual data to provide insightful perspectives into the phenomenon of soil erosion (Doulabian *et al*., 2021; Alitane *et al*., 2022).

Soil erosion is influenced by a multitude of factors, spanning both direct and indirect contributors. These encompass the length and steepness of slopes, rainfall erosivity, the erodibility factor of the soil, crop management practices, and conservation strategies (Wang *et al.*, 2022).

Figure 1: *Study area location with respect to Pakistan.*

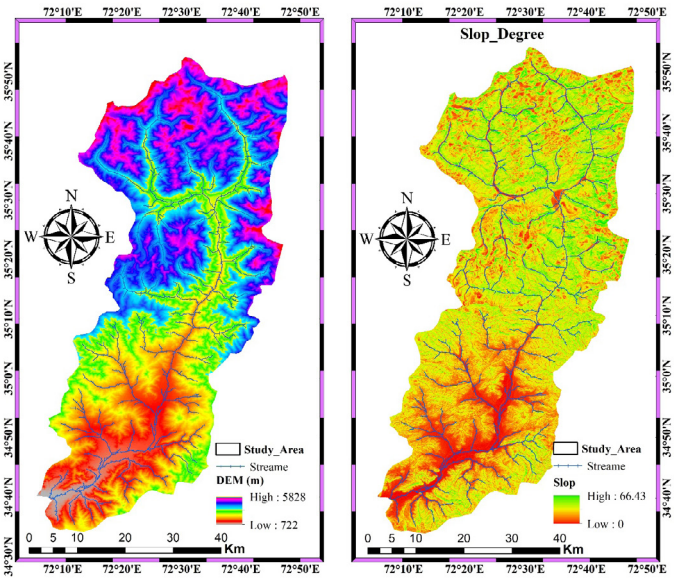

Figure 2: *Digital elevation model and slop of the study area.*

To investigate soil erosion, this research integrated satellite imagery to craft a land cover map, taking into account soil types and agricultural practices. Subsequently, the RUSLE model was applied to this dataset, capitalizing on its compatibility with Geographic Information Systems (GIS) to enhance precision in analysis. The RUSLE equation (Equation 1) was derived, amalgamating five input factors sensitive to spatial and temporal fluctuations:

$$A = R \times K \times LS \times C \times P \quad \ldots(1)$$

Here, (A) signifies the annual soil erosion rate (t ha–1 y–1), (R) represents the rainfall erosivity factor (MJ mm ha–1 h–1 y–1), (K) denotes the soil erodibility factor (t ha–1 MJ–1 ha–1 MM–1), while the remaining parameters are dimensionless. By individually integrating these five components, empirical estimations of soil erosion were undertaken utilizing the raster map tool within ArcGIS. The analysis and processing of all spatial data, including the delineation of the study region, were facilitated using ArcGIS 10.8. Table 1 displays the estimated RUSLE parameters and the corresponding data source.

Table 1: *Dataset sources.*

Data	Spatial resolution	Data source
Rainfall data	Monthly average rainfall data	Pakistan meteorological department
Digital elevation model (DEM)	30 m	STRM
Soil data	Global FAO soil map of 5×5	Food and agriculture organization
Land cover	10m	Sentinel 2 data

R factor

The component concerning annual precipitation holds significant importance in delineating the overall amount and intensity of rainfall. To gather this crucial data, monthly precipitation records spanning a decade (2012-2022) were procured from the Pakistan Meteorological Department for each of the five weather stations within the study area. Nevertheless, estimating this factor encountered certain challenges owing to specific data prerequisites. To overcome these challenges, streamlined procedures were formulated. The annual precipitation data, measured in millimetres, are fundamental for computing rainfall's erosivity factor (R). Consequently, regions with higher annual precipitation exhibit elevated R-values. This insight aids in determining the R factor by leveraging the average annual rainfall value. In the pursuit of mapping rainfall across the research

area, the Inverse Distance Weighting (IDW) method was employed through ArcMap. This technique holds a well-established reputation as one of the most efficacious tools for predicting precipitation patterns across a designated geographical expanse (Maleika, 2020; Liu *et al*., 2020). Numan (Ejaz *et al*., 2023) introduces an Equation that has been acknowledged as the most accurate means of calculating the R factor.

$$R = -8.12 + 0.562 \times PCP \quad \ldots (2)$$

Here, PCP signifies the average annual precipitation in millimetres. This equation facilitates a precise determination of the rainfall's erosivity factor, contributing to the comprehensive understanding of erosive forces at play.

LS factor

Within this study, the variables L and S within the RUSLE model encapsulate the influence of topography on erosion rates. It's recognized that soil erosion and overland flow tend to intensify with greater slope length and steepness (Siswanto and Sule, 2019). Interestingly, alterations in slope length exert a more substantial impact on total soil loss compared to changes in the slope's angle or inclination (McCool *et al*., 1987). The ground slope surpassing the critical angle emerges as a pivotal determinant in soil erosion dynamics. Our research harnessed the Digital Elevation Model (DEM) within the ArcGIS framework to calculate the LS (length and steepness) value. This value furnishes intricate insights into the distribution of slope length and steepness across the terrain.

The calculation of LS integrates both flow accumulation and slope steepness. We derived the runoff accumulation rate and slope characteristics by amalgamating these factors through the ArcGIS Spatial Analyst add-on. To derive the LS factor for our analysis, we employed Equation 3, as introduced by Moore and Burch (1986).

$$LS = \frac{(\text{Flow accumulation} \times \text{CellSize})^{0.4}}{22.13} \times \frac{(\text{SinSlope})^{1.3}}{0.0896} \quad \ldots (3)$$

Here, flow accumulation corresponds to the aggregate upslope supporting area of the grid cell. The LS Factor signifies the amalgamation of slope length and steepness. The variable cell size reflects the dimension of a singular grid cell, while 'Sin slope' encapsulates the degree of slope in terms of sine. This equation serves as a foundational element in our analysis, contributing to a nuanced comprehension of the role of topography in soil erosion patterns.

K factor

The K Factor serves as a quantitative measure of the ease with which soil particles detach from their parent soil and are transported away by rainfall and runoff. It is primarily influenced by the soil's texture, organic matter content, structure, and permeability. SE, denoting the "rate of erosion per unit of the erosion index from a typical unit plot of 22.13 meters in length with a slope gradient of 9%" (Ganasri and Ramesh, 2016), reflects the pace of soil loss corresponding to the erosivity of rainfall (R) index.

Originally, the equation proposed by Wischmeier and Smith (1978), requiring insights into soil structure and permeability, was solved using the formulation provided by Sharpley and Williams (1990). This facilitated the estimation of soil erodibility. The subsequent Equation 4 breaks down the calculation of the K_Factor:

$$K = Fcsand * Fsi - cl * \text{Forgc} * \text{Fhisand} * 0.1317 \quad \ldots (4)$$

Where; Fcsand indicates the influence of coarse sand content on erodibility. Higher amounts of coarse sand correspond to lower erodibility, while greater fine sand content leads to higher values. Fsi represents the effect of the ratio between clay and silt on erodibility. Higher clay-to-silt ratios result in lower erodibility. Forgc accounts for the reduction of erosion in soils rich in organic matter. Fhisand signifies that erosion decreases in soils with a high proportion of sand.

These factors collectively shape the K factor, allowing for a more nuanced understanding of how soil properties influence its susceptibility to erosion. The variable 'C' stands for the percentage of organic matter content, 'SN1' signifies the sand content, while 'CLA', 'SIL', and 'SAN' denote the proportions of clay, silt, and sand, respectively. This equation encapsulates the intricate relationships between soil characteristics and erosion dynamics, offering insights into erosion vulnerability.

LULC data

To generate the land use and land cover (LULC) map for the Swat District, we employed Sentinel-2 data

processed in ArcGIS. The stacking tool was utilized to combine all satellite images, and subsequently, the "pan-sharpening tool" was applied to enhance the image resolution. To delineate distinct LULC categories, training areas were selected to generate hyperplanes. Machine learning techniques, specifically Support Vector Machines (SVM), were employed for classifying the high-dimensional remote sensing data (Adugna *et al.*, 2022; Balkhair and Rahman, 2021). The accuracy of the LULC classification is commonly assessed using techniques such as the confusion matrix and kappa coefficient (Motlagh *et al.*, 2020; Parida and Mandal, 2020). A multivariate, discrete method known as Kappa analysis was used to evaluate the accuracy and precision of the generated LULC maps. Accuracy analysis included total accuracy, producer, and user accuracy, and overall kappa coefficient.

The user's accuracy was determined by dividing the total image pixels by correctly classified pixels for every LULC class. The producer's accuracy was obtained by dividing the number of correct pixels in every LULC class by the total number of pixels in the reference points. The formula for calculating total accuracy is:

$$Overall\ Accuracy = \frac{Total\ number\ of\ correctly\ classified\ pixcel}{Total\ Number\ of\ refferences\ pixels} \times 100 \quad ...(5)$$

The observed image's Kappa factor was used to evaluate accuracy.

The Kappa coefficient represents a classification technique's relative error reduction relative to random categorization. A Kappa value 1 indicates perfect agreement, whereas 0.811 means the LULC map reduces 81.1% of errors. The below Equation 6 was used to calculate the Kappa coefficient for several categorization techniques.

$$Kappa\ Cofficient\ (T) = \frac{(TS \times TCS) - \sum(Column\ total \times Row\ total)}{TS2 - \sum(Column\ total - Row\ total)} \times 100 \quad ...(6)$$

TS= Total samples; TCS= Total corrected samples.

C factor

When it comes to assessing soil loss, Land Use and Land Cover (LULC) classifications play a pivotal role through the C factor. Calculating the C factor involves incorporating information about soil management, crop type, soil moisture, and variations in soil surface conditions. However, evaluating these characteristics can be challenging due to data limitations and the multitude of potential combinations (Farhan and Nawaiseh, 2015). In this study, we leveraged LULC categorization to determine the C factor, adhering to the guidelines outlined by (Yesuph and Dagnew, 2019). Utilizing the LULC map of the basin, we derived the C parameter. To translate this into practice, we followed a literature-recommended approach, as proposed by (Swarnkar *et al.*, 2018; Maqsoom *et al.*, 2020; Allafta and Opp, 2022), where we transformed the raster map into a vector format to represent the corresponding C factor for each LULC category. Table 2 presents a comprehensive compilation of values for the cover management factor, spanning from 0 to 1. This C factor is crucial in soil erosion modeling, as it estimates an area's susceptibility to soil loss. In essence, higher C-factor values within this table indicate greater vulnerability to soil erosion in the corresponding areas. This signifies that region with elevated C-factor values tend to possess less effective vegetation cover or management practices, rendering them more prone to the adverse effects of soil erosion processes. This insight underscores the significance of C-factor assessment in predicting and managing soil erosion dynamics.

Table 2: *C factor for LULC classes.*

S. No	Land cover	C_Factor
1	Grass land	0.7
2	Forest cover	0.004
3	Water bodies	0
4	Crop land	0.65
5	Buildup area	0
6	Snow cover	0
7	Bare land	1

P factor

In soil erosion modeling, the P-factor plays a pivotal role by gauging the efficacy of erosion control practices in curtailing soil loss under particular topographic conditions, especially those involving up-and-downhill ploughing. This factor considers an array of land treatments and interventions designed to curtail the movement of soil particles and mitigate erosion. Practices such as contouring, compaction, constructing sediment basins, and implementing erosion control structures all determine the effectiveness of erosion control measures, thereby influencing the P-factor. In the context of Pakistan, limited endeavours have been made to implement comprehensive erosion control practices, resulting in

a dearth of well-established erosion control measures across the region. Consequently, for the entirety of the study area, the P-factor was ascribed a value of 1. This value signifies the absence of specific erosion control practices and the region's limited resistance against soil erosion. This situation underscores the need for heightened attention and action towards implementing erosion control strategies to mitigate soil erosion's adverse effects (Maqsoom *et al.*, 2020; Batool *et al.*, 2021).

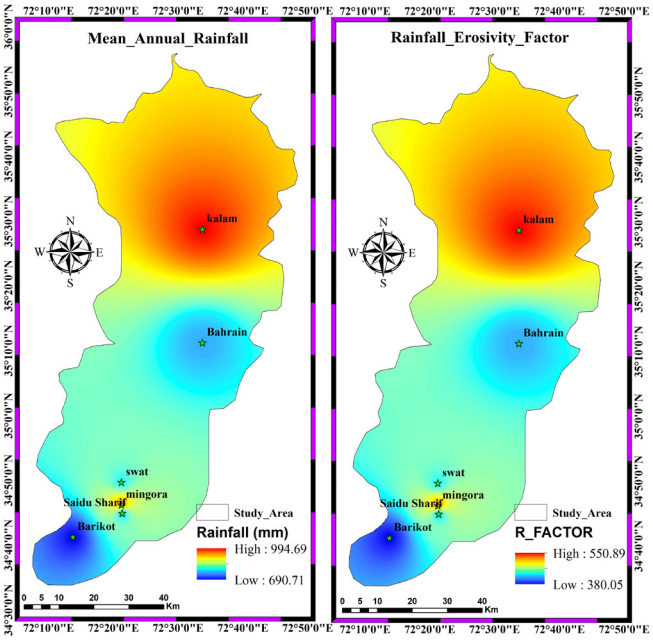

Figure 3: *Rainfall and erosivity factor.*

Results and Discussion

Rainfall erosivity

We leveraged the mean annual rainfall data from various weather stations to generate the R-factor map for the Swat district (Figure 3). The Interpolation technique, Inverse Distance Weighting (IDW), was employed to estimate and interpolate the rainfall values across the entire study area. This process facilitated the creation of a comprehensive R-factor map, showcasing the spatial distribution of erosivity potential. Figure 4 visually presents this spatial distribution, portraying a range of R-factor values spanning from 380 to 550 MJ mm/ha/h/year across the Swat district. This map effectively communicates the variability in erosivity potential, offering insights into how different locations within the study area experience varying levels of erosive forces due to rainfall. This information is crucial for making informed decisions about soil conservation, land management, and erosion prevention strategies in areas that may be more susceptible to soil erosion due to higher erosivity values. The R-factor map highlights that the region of Kalam exhibits the highest R-values, indicating a higher potential for erosivity due to the significant amount of rainfall in that area. Conversely, Mingora and Barikot are marked by the lowest R-factor values, suggesting relatively lower erosivity potential in these locations due to lower annual rainfall amounts. This distribution of R-factor values aligns with the local rainfall patterns, with Kalam experiencing higher rainfall compared to Mingora and Barikot. The varying R-factor values across these regions underscore the importance of considering local climate conditions and erosivity potential when implementing erosion control and soil management strategies

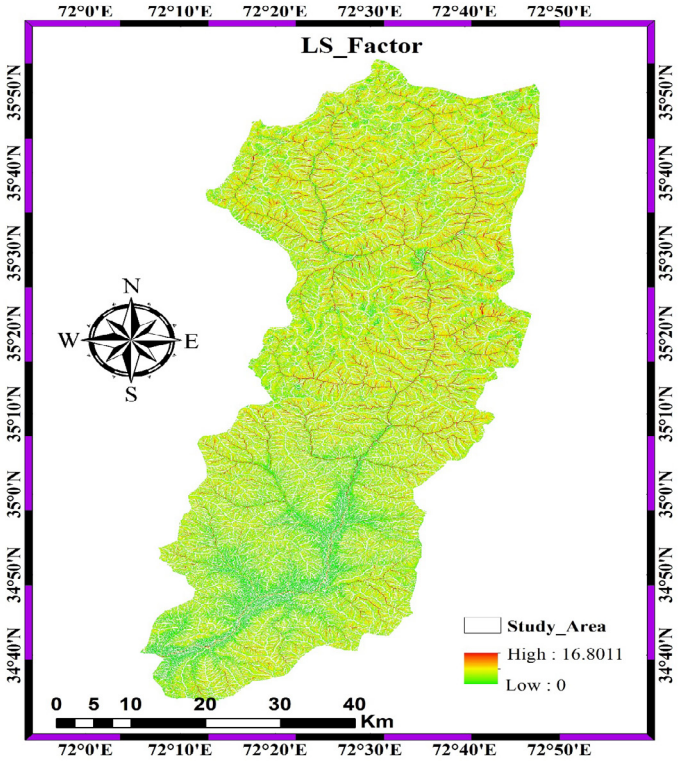

Figure 4: *LS factor map.*

Topographic LS factor

The LS factor map offers valuable insights into how the combination of slope length and gradient contributes to the process of soil erosion. In regions characterized by high LS values, which are primarily concentrated in the northern parts and some southern areas, the influence of steep terrain on soil loss becomes evident.

Figure 2 visually depicts the landscape and reveals an elevation range spanning from 722 to 5828 meters. In areas with steep slopes or elevated LS factor values, a heightened susceptibility exists to moderate to

severe soil erosion. The map effectively communicates that the LS factor varies from 0 to 16 across most of the study area. In regions where LS values approach or reach 16, a moderate to high potential exists for erosive forces, signifying a greater likelihood of soil erosion occurring in those specific areas. As illustrated in Figure 4, the LS factor map provides a visual representation of these findings, shedding light on the distribution of soil erosion susceptibility based on slope characteristics. This information holds significant implications for land management decisions and erosion prevention strategies, especially in regions with high LS factor values that may require targeted interventions to minimize soil loss.

Soil erodibility K factor

The regional distribution of K values in the SWAT region is shown in Figure 5; the values range from 0.24 to 0.33. These values indicate low-to-moderate soil erodibility in the study area. The K factor is further classified into lithosols, Gleysol, and eutriccambisolo. In the map, blue represents areas with low erosion capacity, while yellow indicates high erosion capacity. The gradient from blue to yellow reflects increasing soil erosion potential. The map provides valuable insights into the variation of K values and the associated soil erodibility across different soil types in SWAT. The K factor for lithosols is 0.27, indicating moderate soil erodibility. The K factor for Gleysol is 0.33, suggesting a relatively higher soil erodibility than lithosols. The K factor for eutriccambisolo is 0.24, indicating a lower soil erodibility than the other two soil types.

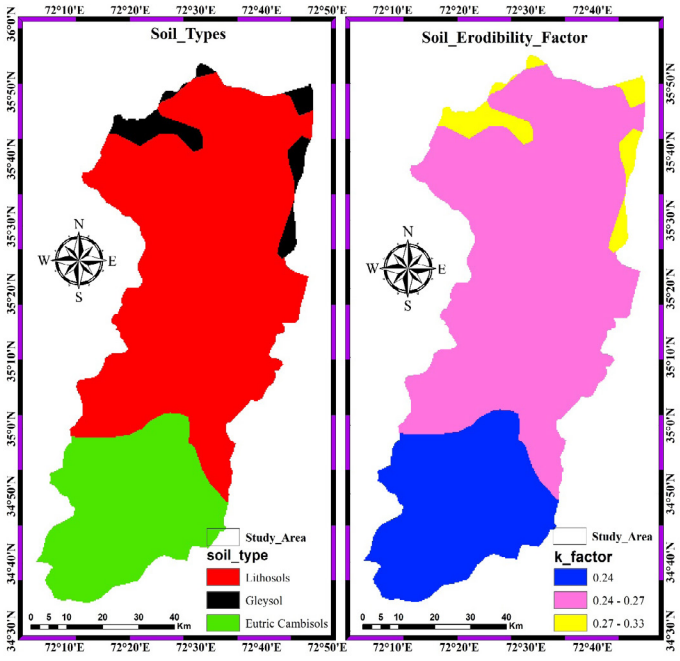

Figure 5: *Soil types and associated K values.*

Land use land cover C factor

Figure 6 visually depicts the Land Use and Land Cover (LULC) classification for the Swat region. This classification categorizes the landscape into seven distinct classes: Bare land, built-up areas, water bodies, natural trees, cropland, snow, and grassland. Each category's regional distribution is clearly illustrated, highlighting their respective proportions. Notably, bare land occupies 12% of the area, built-up areas cover 11%, water bodies account for 1%, natural trees encompass 16%, cropland constitutes 3%, snow is observed on 1%, and the dominant category is grassland, covering an extensive 43% of the entire region.

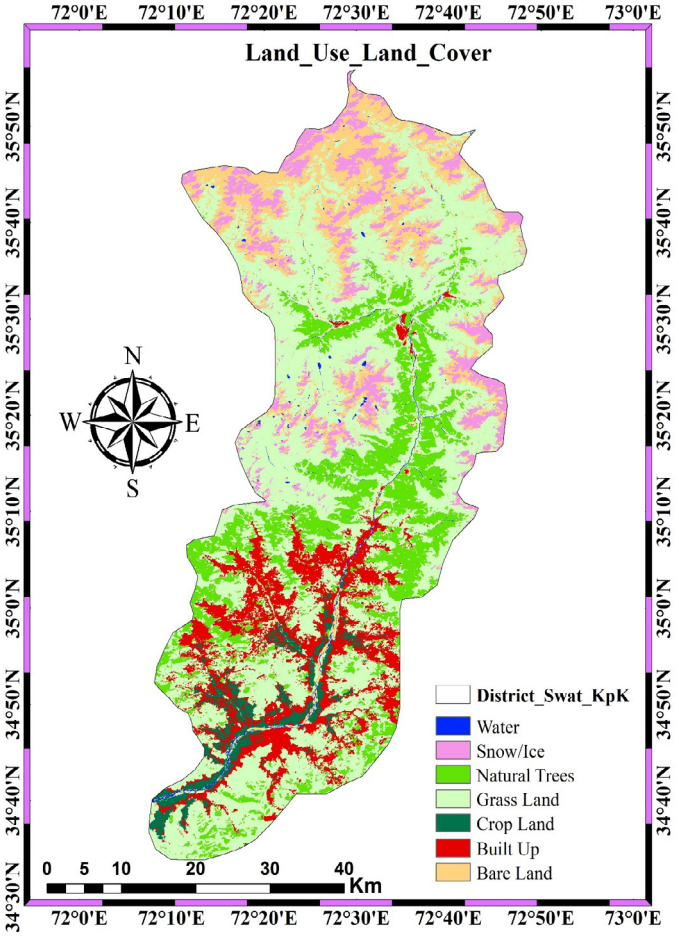

Figure 6: *Land use land cover classes.*

Figure 7, on the other hand, offers insight into the C-factor values associated with the various LULC classes. The C-factor, which assesses the effectiveness of erosion control practices, varies across different land cover categories. This figure visually represents the distribution of C-factor values across the LULC classes, clearly understanding how different land management practices impact soil erosion susceptibility.

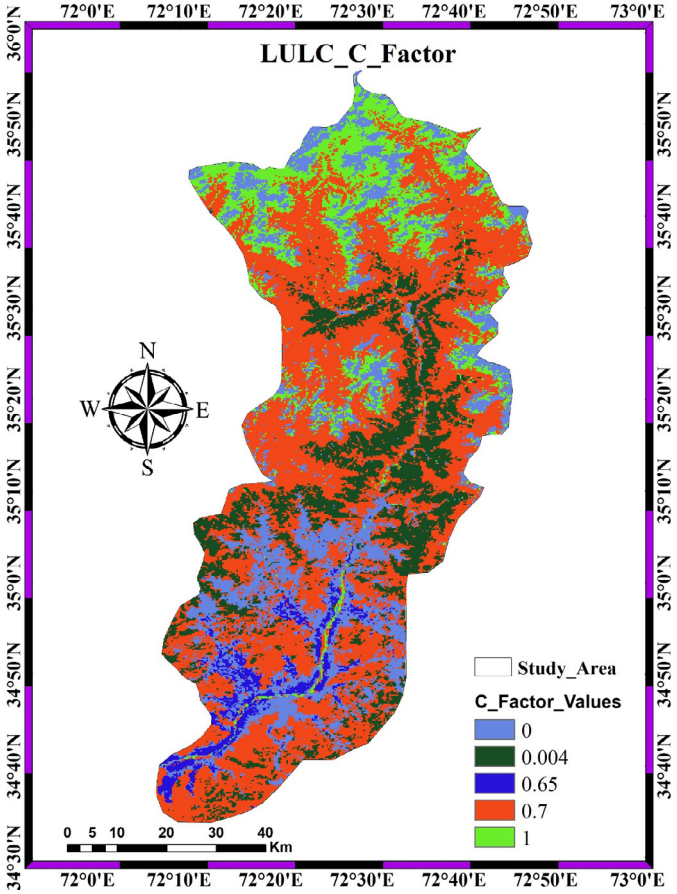

Figure 7: *Land use land cover factor (C_factor).*

The Kappa coefficient was employed as a benchmark to evaluate the accuracy of this land cover classification. The classification process, executed using the Support Vector Machines (SVM) algorithm, yielded an impressive overall accuracy rate of 89%. This substantial level of accuracy reflects a strong agreement between the classified pixels and the ground truth samples, attesting to the reliability of the classification results. The Kappa coefficient, which goes beyond chance agreement, also stands at 0.87. This robust value underscores the high accuracy of the classification outcomes, establishing confidence in the methodology employed. For a more comprehensive understanding of the classification accuracy, detailed information is available in Table 3.

Soil loss estimation

The examination of soil erosion patterns (Figure 8) within the study region uncovered notable spatial discrepancies, underscoring the need for the classification of areas according to their soil erosion occurrences, which facilitates a more structured analysis. Accurate assessment of soil erosion hazards is paramount in identifying regions with heightened risk and devising effective strategies for prevention. In this context, this study adopted a classification system consistent with the OECD standards, a methodology commonly employed in similar regional studies. This classification approach has been utilized in previous research conducted in the same geographic area (Farhan and Nawaiseh, 2015; Aslam *et al.*, 2020).

The classification process involved categorizing erosion rates into five distinct categories (Figure 9) for better understanding and discussion. These categories include very low (less than 1 t ha^{-1} yr^{-1}), low (1-5 t ha^{-1} yr^{-1}), moderate (5-10 t ha^{-1} yr^{-1}), high (10-50 t ha^{-1} yr^{-1}), and extreme (greater than 50 t ha^{-1} yr^{-1}) erosion rates. By employing this classification system, we could assess the magnitude of soil erosion risks across the study area and identify areas that require particular attention and intervention.

Table 3: *LULC accuracy assessment.*

Land cover	Weter	Natural trees	Crop land	Built-up	Bare land	Snow/ Ice	Grass land	Total	User's accuracy
Water	14	1	0	0	1	0	0	16	87.5
Natural trees	0	27	2	0	0	1	1	31	87.09
Crop land	0	1	29	1	1	2	1	35	82.85
Built-up	0	0	1	29	2	0	0	32	90.63
Bare land	1	1	0	1	35	0	1	39	89.74
Snow/Ice	0	1	1	0	0	34	0	36	94.44
Grass land	0	1	2	0	0	0	32	35	91.43
Total	15	32	35	31	39	37	35	224	
Producer's accuracy	93.33	84.38	82.86	93.55	89.74	91.89	91.43		
Koppa	0.87								
Overall accuracy	89%								

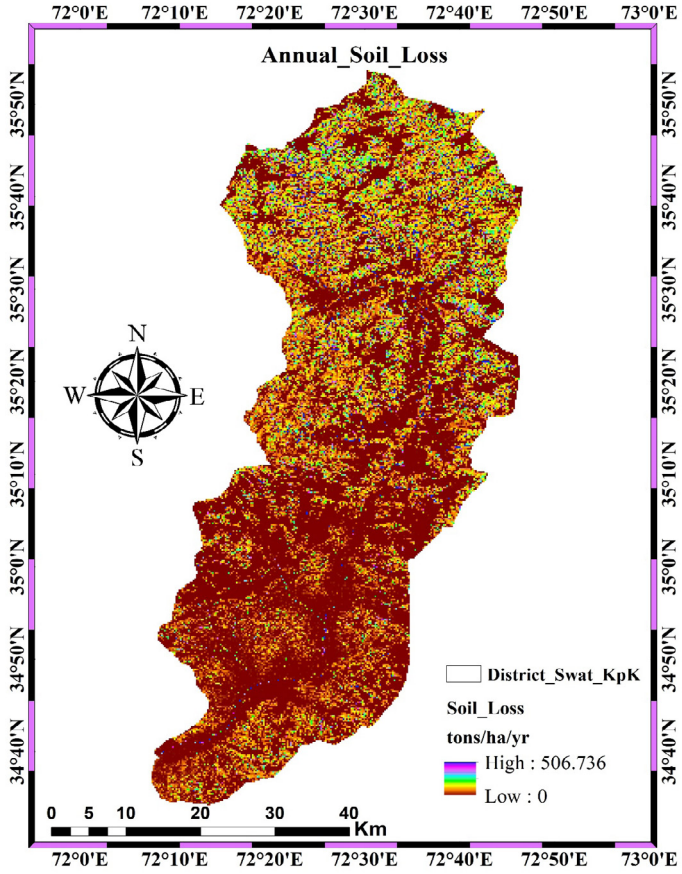

Figure 8: *Soil erosion map for study region.*

This study aimed to ascertain the annual soil erosion rate in the Swat district through the analysis of available geospatial data. Revised Universal Soil Loss Equation (RUSLE) model was utilized due to its cost-effectiveness and practicality in estimating soil erosion. By incorporating RUSLE parameters into Equation 1 with the utilization of spatial analyst tools within ArcGIS, soil erosion risk maps were generated. Figure 8 illustrates the distribution of annual soil loss, from 0 to 506 tons per hectare. The map aptly reveals the spatial disparities in soil erosion, with certain areas exhibiting low soil loss rates juxtaposed with others manifesting higher rates of soil loss. Notably, regions characterized by bare land and steep topography demonstrate heightened susceptibility to soil erosion, as the map indicates.

To provide a more comprehensive elucidation of the soil erosion estimation map, Figure 9 employs Geographic Information System (GIS) techniques to elucidate the soil severity classes specific to the Swat district. These GIS techniques empower an in-depth analysis and visualization of the intricate soil erosion patterns in the study area. By employing advanced geospatial methods, this research sheds light on the complicated dynamics of soil erosion across diverse landscapes within the Swat district, thereby contributing to a more informed understanding of erosion susceptibility and supporting the formulation of targeted land management strategies.

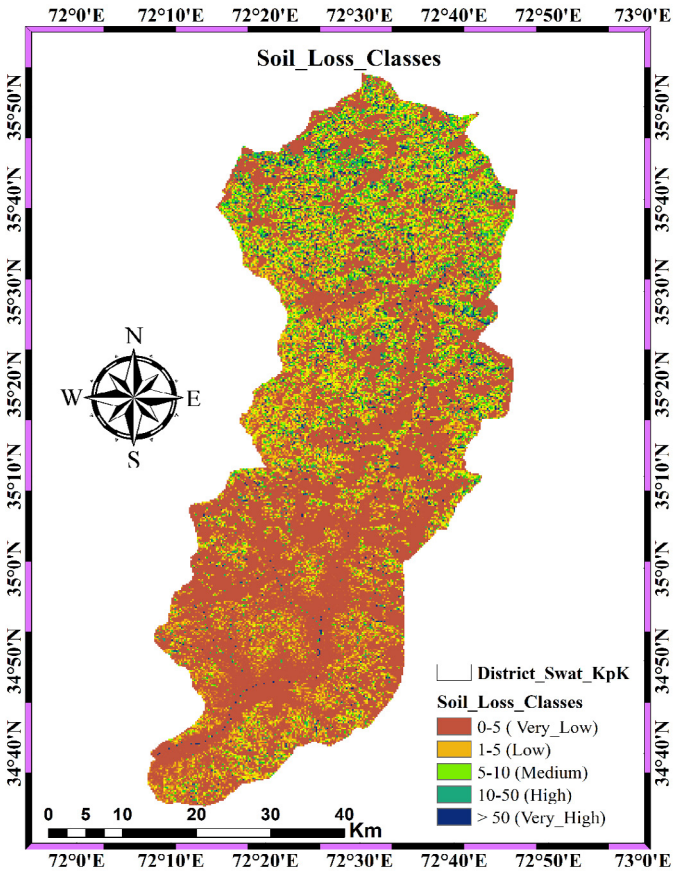

Figure 9: *Soil severity classes based on soil loss.*

Figure 9 illustrates the distribution of soil erosion categories based on the severity map. The study divided the area into five classes to assess erosion risk. The largest portion, 65%, falls under very low erosion, indicating minimal concern. Low covers 16%, suggesting slightly higher risk. Moderate comprises 13%, indicating moderate risk. About 4% is high risk, needing attention. Extreme risk represents 2%, requiring immediate action. This categorization aids land management and conservation planning by prioritizing erosion control efforts effectively. The distribution of soil erosion risk categories, as outlined in Table 4, furnishes essential insights for informed land management and conservation planning.

Table 4: *Soil erosion classification.*

Range	Area%	Classes
0-1 t ha^{-1} yr^{-1}	65%	Very Low
1-5 t ha^{-1} yr^{-1}	16%	Low
5-10 t ha^{-1} yr^{-1}	13%	Medium
10-50 t ha^{-1} yr^{-1}	4%	High
>50 t ha^{-1} yr^{-1}	2%	Extreme

Soil erosion presents a significant and alarming challenge, especially within the studied region, where a combination of factors accelerates the loss of soil and sediment. Factors such as steep terrain, climatic conditions, water flow speed, and environmental elements collectively contribute to elevated runoff rates and sediment deposition. Notably, melting glaciers due to rising global temperatures further exacerbates this susceptibility to erosion. This accelerated glacier melting intensifies the problem of soil erosion in the area. Both natural forces and human activities contribute to soil erosion, highlighting the essential need to assess its severity and identify its underlying causes before implementing corrective measures (Tsegaye and Bharti, 2021).

In the pursuit of quantifying soil erosion across different spatial scales, researchers worldwide have developed various models. When evaluating soil loss and sediment movement, the Revised Universal Soil Loss Equation (RUSLE) is the industry standard (Maqsoom *et al.*, 2020). The RUSLE model is acclaimed for its accuracy in predicting soil loss and considers vital variables like rainfall erosivity, soil erodibility, and land use and land cover (LULC) factors (Tadesse *et al.*, 2017). This study's spatial maps illustrating RUSLE characteristics were meticulously crafted to enhance the reliable estimation of soil erosion rates. By utilizing these independently constructed maps, the research enhances the precision of soil erosion rate calculations, contributing to a more nuanced comprehension of this crucial concern.

RUSLE has garnered extensive recognition among academia and researchers as a dependable and efficient technique for assessing soil loss. Nonetheless, challenges stemming from data availability and resource constraints have impeded the practical validation of its outcomes (Maqsoom *et al.*, 2020). Nevertheless, the findings of this study harmonize with prior research conducted in the neighboring vicinity. For example, within the Fateh Jang watershed, uncultivated areas exhibited annual soil losses ranging from 17 to 41 tonnes per hectare, while cultivated land displayed comparatively lower rates of 9 to 26 tonnes per year (Ullah *et al.*, 2018). Another study utilizing RUSLE to gauge soil loss in a hilly terrain reported rates spanning from 0.1 to 8.0 tons per hectare annually, with an average of 19.1 tons per hectare annually across a 13-hectare expanse, where steep slopes contributed to 74% of the erosion (Nasir *et al.*, 2006). In a different investigation, an average soil loss of 92.6 million tonnes was identified, with the Chakwal watershed presenting 70.06% low erosion, 16.51% intermediate erosion, and 13.44% highly eroded zones (Batool *et al.*, 2021). In a study conducted within the Kashmir region, soil erosion maps were classified into four categories: low (0-1), medium (1–5), high (5–20), and very high (>20), revealing an annual soil loss rate of 22.25 tonnes per hectare (Gilani *et al.*, 2022). Moreover, when compared to the average erosion rate reported in Pakistan's Chitral region, Swat exhibited significantly lower soil erosion rates, with the Chitral region recording a rate of 78 tons per hectare per year (Maqsoom *et al.*, 2020). These aligned findings underscore the applicability and validity of the RUSLE methodology across diverse geographical contexts, aiding in a more comprehensive understanding of soil erosion dynamics.

The assessment of soil erosion plays a pivotal role in addressing the challenges posed by extensive sedimentation and shifts in land use patterns. This evaluation holds particular importance in establishing enduring infrastructure that facilitates water harvesting, ensuring a consistent water supply even during arid periods. Notably, the impact of deforestation exacerbates the gravity of soil erosion. Moreover, this assessment contributes to mitigating soil erosion within the researched area. Recognizing the significance of this issue, the Khyber Pakhtunkhwa (KPK) government has taken proactive measures such as tree planting and strip farming as conservation practices aimed at curbing soil loss in the region. These initiatives demonstrate a concerted effort towards sustainable land management and effective erosion control.

Conclusions and Recommendations

In this study, we harnessed the power of the Revised Universal Soil Loss Equation (RUSLE) empirical model in conjunction with cutting-edge Remote Sensing (RS) and Geographic Information System (GIS) techniques to delve into the intricate landscape of soil loss rates within the Swat district. The adoption of the RUSLE model was driven by its simplicity, data efficiency, and capacity to facilitate actionable insights. Our comprehensive analysis, fusing RS, GIS, and RUSLE, enabled us to evaluate soil losses quantitatively, categorizing the basin area into five

distinct vulnerability groups predicated on their predisposition to soil erosion.

The findings we unearthed cast a spotlight on a critical concern: The Swat district, particularly its northern reaches encompassing Kalam, Bahrain, and Pashmal, emerges as a hotspot for severe soil erosion. The gravity of vulnerability in these locales demands urgent attention. With an average soil loss of 31.25 tonnes per hectare per year and substantial erosion observed in these designated pockets, the present erosion rates represent a tangible threat to land integrity if unattended. The 2% of land grappling with extreme soil erosion demands immediate intervention and strategic measures to ensure the preservation of land utilization dynamics and safeguard the well-being of local communities. The far-reaching implications of substantial sediment generation ripple through the existing drainage systems in the region. Our furnished dataset, intricately delineating erosion severity classes and intensity, guides policymakers and planners to choreograph tailored strategies in sync with specific erosion profiles.

Furthermore, the harmonious fusion of GIS with the RUSLE model presents an unwavering foundation for deciphering, addressing, and curbing soil erosion across expansive landscapes. This amalgamation empowers soil conservation agencies to calibrate their focus and resources toward regions with heightened vulnerability, heralding a proactive approach to land preservation. As the curtain draws on this research endeavor, our gaze turns toward a future horizon, one that beckons for a deeper understanding of the multifaceted contributors to soil erosion land use dynamics, rainfall patterns, and vegetative influences. This knowledge is pivotal in sculpting precision-engineered solutions poised to stand as bulwarks against the relentless forces of erosion. As we conclude this chapter, the torch of inquiry continues to burn, illuminating pathways toward sustainable land management practices, a pursuit we entrust to future researchers and guardians of our precious terrestrial ecosystem.

This study emphasises on the availability of Open-source data, which were utilized to for the soil loss assessments through the RUSLE model. However, it's noteworthy that due to the coarser resolution of the freely available data, certain limitations were inherent in the accuracy and precision of the model's predictions. The Digital Elevation Model (DEM) data and land cover information used, though beneficial, were constrained by their spatial resolutions that underpin the estimation of terrain features and land use dynamics that significantly influence soil loses. Several recommendations are proposed to address these limitations and improve the study. At first, field validation using actual soil loss measurements from representative areas within the investigation zone will validate the model's predictions and facilitate its calibration for more precision. Moreover, integrating higher-resolution DEM data (1-5m), drone imagery with a spatial resolution (2-3cm) may provide a more detailed understanding of terrain complexities and enhance the accuracy of slope-related calculations. Similarly, incorporating high-resolution land cover data derived from drone imagery can offer a finer-grained depiction of land use changes and conservation efforts, ultimately leading to more accurate soil loss assessments. By leveraging drone-based imagery, the study can monitor the dynamic variations in vegetal cover over temporal scale, highlighting the seasonal impacts on soil erosion. Through sensitivity analysis with this high-resolution data, critical parameters affecting soil loss predictions can be computed, thereby refining the reliability and applicability of the soil loss assessments.

Novelty Statement

The novelty of RUSLE model provides seasonal dynamics of precipitation by considering rainfall and vegetated areas along with the land use land cover spatial-temporal variations. As the swat watershed is enlarged scale watershed having the 5337 km^2 area which need the reliability of RUSLE outputs.

Author's Contribution

Sumaira Kousar: Conceptualization, Methodology, Software, Validation, formal analysis and original draft preparation.
Safdar Ali Sherazi: Final review and editing.

Conflicts of interest
The authors have declared no conflict of interest.

References

Adugna, T., W. Xu and J. Fan. 2022. Comparison

of random forest and support vector machine classifiers for regional land cover mapping using coarse resolution FY-3C images. Remote Sens., 14(3): 1–22. https://doi.org/10.3390/rs14030574

Alewell, C., B. Ringeval, C. Ballabio, D.A. Robinson, P. Panagos and P. Borrelli. 2020. Global phosphorus shortage will be aggravated by soil erosion. Nat. Commun., 11(1). https://doi.org/10.1038/s41467-020-18326-7

Alitane, A., A. Essahlaoui, M. El-Hafyani, A. El Hmaidi, A. El-Ouali, A. Kassou and A. Van Rompaey. 2022. Water Erosion monitoring and prediction in response to the effects of climate change using RUSLE and SWAT equations: Case of R'Dom watershed in Morocco. Land, 11(1). https://doi.org/10.3390/land11010093

Allafta, H. and C. Opp. 2022. Soil erosion assessment using the RUSLE model, remote sensing, and GIS in the Shatt Al-Arab Basin (Iraq-Iran). Appl. Sci. (Switzerland), 12(15). https://doi.org/10.3390/app12157776

Amundson, R., A.A. Berhe, J.W. Hopmans, C. Olson, A.E. Sztein and D.L. Sparks. 2015. Soil and human security in the 21st century. Science, 348(6235): 1261071. https://doi.org/10.1126/science.1261071

Ashraf, A., M.K. Abuzar, B. Ahmad, M.M. Ahmad and Q. Hussain. 2017. Modeling risk of soil erosion in high and medium rainfall zones of pothwar region, Pakistan. Proc. Pak. Acad. Sci. B, 54(2): 67–77.

Aslam, B., A. Maqsoom, Shahzaib, Z.A. Kazmi, M. Sodangi, F. Anwar and D. Farooq. 2020. Effects of landscape changes on soil erosion in the built environment: Application of geospatial-based RUSLE technique. Sustainability (Switzerland), 12(15). https://doi.org/10.3390/su12155898

Bacha, M.S., M. Muhammad, Z. Kılıç and M. Nafees. 2021. The dynamics of public perceptions and climate change in Swat valley, Khyber Pakhtunkhwa, Pakistan. Sustainability (Switzerland), 13(8): 1–22. https://doi.org/10.3390/su13084464

Balkhair, K.S. and K. Rahman. 2021. Development and assessment of rainwater harvesting suitability map using analytical hierarchy process, GIS and RS techniques. Geocarto Intl., 36(4): 421–448. https://doi.org/10.1080/10106049.2019.1608591

Bangash, S., 2012. Socio-economic conditions of post-conflict Swat: A critical appraisal. Tigah J. Peace Dev., 2: 66–79.

Batool, S., S.A. Shirazi and S.A. Mahmood. 2021. Appraisal of soil erosion through RUSLE model and hypsometry in Chakwal watershed (Potwar-Pakistan). Sarhad J. Agric., 37(2): 594–606.

Bazzani, F., 2013. Technical assistance and support to fruit and vegetable growers in the Swat Valley (Pakistan) for the improvement of production and marketing in the horticultural value chain" (ADP SWAT) Atlas of the Natural Resources Evaluation in Swat Valley, Khyber Pakhtunkhwa, Islamic Republic of Pakistan.

Boardman, J., 2006. Soil erosion science: Reflections on the limitations of current approaches. Catena, 68(2–3): 73–86. https://doi.org/10.1016/j.catena.2006.03.007

Boardman, J., M.L. Shepheard, E. Walker and I.D.L. Foster. 2009. Soil erosion and risk-assessment for on- and off-farm impacts: A test case using the Midhurst area, West Sussex, UK. J. Environ. Mgt., 90(8): 2578–2588. https://doi.org/10.1016/j.jenvman.2009.01.018

Borrelli, P., D.A. Robinson, L.R. Fleischer, E. Lugato, C. Ballabio, C. Alewell and P. Panagos. 2017. An assessment of the global impact of 21st century land use change on soil erosion. Nat. Commun., 8(1). https://doi.org/10.1038/s41467-017-02142-7

Borrelli, P., D.A. Robinson, P. Panagos, E. Lugato, J.E. Yang, C. Alewell and C. Ballabio. 2020. Land use and climate change impacts on global soil erosion by water (2015-2070). Proc. Natl. Acad. Sci. U.S.A., 117(36): 21994–22001. https://doi.org/10.1073/pnas.2001403117

Bucała, A., A. Budek and M. Kozak. 2015. The impact of land use and land cover changes on soil properties and plant communities in the Gorce Mountains (Western Polish Carpathians), during the past 50 years. Z. Geomorphol., 59(2): 41–74. https://doi.org/10.1127/zfg_suppl/2015/S-59204

Choudhury, B.U., G. Nengzouzam and A. Islam. 2022. Runoff and soil erosion in the integrated farming systems based on micro-watersheds under projected climate change scenarios and adaptation strategies in the eastern Himalayan mountain ecosystem (India). J. Environ. Mgt., 309: 114667. https://doi.org/10.1016/j.

jenvman.2022.114667

Chuenchum, P., M. Xu and W. Tang. 2020. Estimation of soil erosion and sediment yield in the lancang-mekong river using the modified revised universal soil loss equation and GIS techniques. Water (Switzerland), 12(1). https://doi.org/10.3390/w12010135

Dahri, Z.H., B. Ahmad, J.H. Leach and S. Ahmad. 2011. Satellite-based snowcover distribution and associated snowmelt runoff modeling in Swat River Basin of Pakistan. Proc. Pak. Acad. Sci., 48(1): 19–32.

Doulabian, S., A.S. Toosi, G.H. Calbimonte, E.G. Tousi and S. Alaghmand. 2021. Projected climate change impacts on soil erosion over Iran. J. Hydrol., 598(4): 126432. https://doi.org/10.1016/j.jhydrol.2021.126432

Ejaz, N., M. Elhag, J. Bahrawi, L. Zhang, H.F. Gabriel and K.U. Rahman. 2023. Soil erosion modelling and accumulation using RUSLE and remote sensing techniques: Case study Wadi Baysh, Kingdom of Saudi Arabia. Sustainability (Switzerland), 15(4): 1–14. https://doi.org/10.3390/su15043218

El-Jazouli, A., A. Barakat, A. Ghafiri, S. El-Moutaki, A. Ettaqy and R. Khellouk. 2017. Soil erosion modeled with USLE, GIS, and remote sensing: a case study of Ikkour watershed in Middle Atlas (Morocco). Geosci. Lett., 4(1). https://doi.org/10.1186/s40562-017-0091-6

Emadodin, I. and H.R. Bork. 2012. Degradation of soils as a result of long-term human-induced transformation of the environment in Iran: An overview. J. Land Use Sci., 7(2): 203–219. https://doi.org/10.1080/1747423X.2011.560292

FAO, 2011. The state of the World's land and water resources (SOLAW)–Managing systems at risk. http://www.fao.org/3/i1688e/i1688e.pdf

FAO, 2019. Global symposium on soil erosion (GSER 2019): Symposium working documents. https://www.fao.org/publications/card/es/c/CA4394EN/

Farhan, Y., and S. Nawaiseh. 2015. Spatial assessment of soil erosion risk using RUSLE and GIS techniques. Environ. Earth Sci., 74(6): 4649–4669. https://doi.org/10.1007/s12665-015-4430-7

Ganasri, B.P., and H. Ramesh. 2016. Assessment of soil erosion by RUSLE model using remote sensing and GIS. A case study of Nethravathi Basin. Geosci. Front., 7(6): 953–961. https://doi.org/10.1016/j.gsf.2015.10.007

Gayen, A. and S. Saha. 2017. Application of weights-of-evidence (WoE) and evidential belief function (EBF) models for the delineation of soil erosion vulnerable zones: a study on Pathro river basin, Jharkhand, India. Model. Earth Syst. Environ., 3(3): 1123–1139. https://doi.org/10.1007/s40808-017-0362-4

Gilani, H., A. Ahmad, I. Younes and S. Abbas. 2022. Impact assessment of land cover and land use changes on soil erosion changes (2005–2015) in Pakistan. Land Degradation and Devel., 33(1): 204–217. https://doi.org/10.1002/ldr.4138

Hewett, C.J.M., C. Simpson, J. Wainwright and S. Hudson. 2018. Communicating risks to infrastructure due to soil erosion: A bottom-up approach. Land Degrad. Dev., 29(4): 1282–1294. https://doi.org/10.1002/ldr.2900

Islam, F., S. Riaz, B. Ghaffar, A. Tariq, S.U. Shah, M. Nawaz and M. Aslam. 2022. Landslide susceptibility mapping (LSM) of Swat District, Hindu Kush Himalayan region of Pakistan, using GIS-based bivariate modeling. Front. Environ. Sci., 10(4): 1–18. https://doi.org/10.3389/fenvs.2022.1027423

Keesstra, S.D., J. Bouma, J. Wallinga, P. Tittonell, P. Smith, A. Cerdà and L.O. Fresco. 2016. The significance of soils and soil science towards realization of the United Nations sustainable development goals. Soil, 2(2): 111–128. https://doi.org/10.5194/soil-2-111-2016

Khan, S.R., and S.R. Khan. 2009. Assessing poverty-deforestation links: Evidence from Swat, Pakistan. Ecol. Econ., 68(10): 2607–2618. https://doi.org/10.1016/j.ecolecon.2009.04.018

Kheir, R.B., C. Abdallah and M. Khawlie. 2008. Assessing soil erosion in Mediterranean karst landscapes of Lebanon using remote sensing and GIS. Eng. Geol., 99: 239–254. https://doi.org/10.1016/j.enggeo.2007.11.012

Kriegler, E., B.O. Neill, S. Hallegatte, T. Kram, R. Lempert, T.J. Wilbanks and R.H. Moss. 2013. Socio-economic scenario development for climate change analysis. (C.I.R.E.D.) https://hal.science/hal-00866437

Lal, R., 2017. Soil erosion and global warming in India. J. Soil Water Conserv., 16(4): 297. https://doi.org/10.5958/2455-7145.2017.00044.3

Liu, D., Q. Zhao, D. Fu, S. Guo, P. Liu and Y. Zeng.

2020. Comparison of spatial interpolation methods for the estimation of precipitation patterns at different time scales to improve the accuracy of discharge simulations. Hydrol. Res., 51(4): 583–601. https://doi.org/10.2166/nh.2020.146

Maleika, W., 2020. Inverse distance weighting method optimization in the process of digital terrain model creation based on data collected from a multibeam echosounder. Appl. Geomat., 12(4): 397–407. https://doi.org/10.1007/s12518-020-00307-6

Maqsoom, A., B. Aslam, U. Hassan, Z.A. Kazmi, M. Sodangi, R.F. Tufail and D. Farooq. 2020. Geospatial assessment of soil erosion intensity and sediment yield using the revised universal soil loss equation (RUSLE) model. ISPRS Int. J. Geo-Inf., 9(6). https://doi.org/10.3390/ijgi9060356

McCool, D.K., L.C. Brown, G.R. Foster, C.K. Mutchler and L.D. Meyer. 1987. Revised slope steepness factor for the universal soil loss equation. Trans. Am. Soc. Agric. Eng., 30(5): 1387–1396. https://doi.org/10.13031/2013.30576

Meliho, M., A. Khattabi and N. Mhammdi. 2020. Spatial assessment of soil erosion risk by integrating remote sensing and GIS techniques: A case of Tensift watershed in Morocco. Environ. Earth Sci., 79(10). https://doi.org/10.1007/s12665-020-08955-y

Mohammadi, S., H. Karimzadeh and M. Alizadeh. 2018. Spatial estimation of soil erosion in Iran using RUSLE model. Iran. J. Ecohydrol., 5(2): 551–569.

Moore, I.A.N.D., and G.J. Burch. 1986. Division S-6-soil and water management physical basis of the length-slope factor in the universal soil loss equation 1. Soil Conserv., 50(1986): 1294–1298. https://doi.org/10.2136/sssaj1986.03615995005000050042x

Moore, I.D., and G.J. Burch. 1986. Modelling erosion and deposition: Topographic effects. Trans. Am. Soc. Agric. Eng., 29(6): 1624–1630. https://doi.org/10.13031/2013.30363

Morgan, R.P.C., 2001. A simple approach to soil loss prediction: A revised morgan-morgan-finney model. Catena, 44(4): 305–322. https://doi.org/10.1016/S0341-8162(00)00171-5

Motlagh, Z.K., A. Lotfi, S. Pourmanafi, S. Ahmadizadeh and A. Soffianian. 2020. Spatial modeling of land-use change in a rapidly urbanizing landscape in central Iran: Integration of remote sensing, CA-Markov, and landscape metrics. Environ. Monit. Assess., 192(11). https://doi.org/10.1007/s10661-020-08647-x

Nasir, A., K. Uchida and M. Ashraf. 2006. Estimation of soil erosion by using RUSLE and GIS for Small mountainous watersheds in Pakistan. Pak. J. Water Resour., 10(1): 11–21.

Nearing, M.A., V.O. Polyakov, M.H. Nichols, M. Hernandez, L. Li, Y. Zhao and G. Armendariz. 2017. Slope-velocity equilibrium and evolution of surface roughness on a stony hillslope. Hydrol. Earth Syst. Sci., 21(6): 3221–3229. https://doi.org/10.5194/hess-21-3221-2017

Nekhay, O., M. Arriaza and L. Boerboom. 2009. Evaluation of soil erosion risk using analytic network process and GIS: A case study from Spanish mountain olive plantations q. J. Environ. Mgt., 90(10): 3091–3104. https://doi.org/10.1016/j.jenvman.2009.04.022

Parida, B.R., and S.P. Mandal. 2020. Polarimetric decomposition methods for LULC mapping using ALOS L-band PolSAR data in western parts of Mizoram, Northeast India. SN Appl. Sci., 2(6): 1–15. https://doi.org/10.1007/s42452-020-2866-1

Qasim, M., K. Hubacek, M. Termansen and L. Fleskens. 2013. Modelling land use change across elevation gradients in district Swat, Pakistan. Reg. Environ. Change, 13(3): 567–581. https://doi.org/10.1007/s10113-012-0395-1

Robinson, D.A., P. Panagos, P. Borrelli, A. Jones, L. Montanarella, A. Tye and C.G. Obst. 2017. Soil natural capital in Europe; A framework for state and change assessment. Sci. Rep., 7(1): 1–14. https://doi.org/10.1530/jrf.0.0890001

Sandeep, P., K.C.A. Kumar and S. Haritha. 2021. Risk modelling of soil erosion in semi-arid watershed of Tamil Nadu, India using RUSLE integrated with GIS and remote sensing. Environ. Earth Sci., 80(16): 1–20. https://doi.org/10.1007/s12665-021-09800-6

Sharpley, A.N., and J.R. Williams. 1990. EPIC: The erosion-productivity impact calculator. U.S. Dep. Agric. Tech. Bull., 1768: 235. http://agris.fao.org/agris-search/search.do?recordID=US9403696

Siswanto, S.Y., and M.I.S. Sule. 2019. The impact of slope steepness and land use type on soil properties in Cirandu Sub-Sub

Catchment, Citarum Watershed. IOP Conf. Ser. Earth Environ. Sci., 393(1). https://doi.org/10.1088/1755-1315/393/1/012059

Swarnkar, S., A. Malini, S. Tripathi and R. Sinha. 2018. Uncertainty in soil erosion and sediment yield modelling India. pp. 2471–2485. https://doi.org/10.5194/hess-22-2471-2018

Tadesse, L., K.V. Suryabhagavan, G. Sridhar and G. Legesse. 2017. Land use and land cover changes and Soil erosion in Yezat Watershed, North Western Ethiopia. Int. Soil Water Conserv. Res., 5(2): 85–94. https://doi.org/10.1016/j.iswcr.2017.05.004

Tongde, C., F. Abbas, J. Juying, S.S. Ijaz, A. Shoshan, M. Ansar and A. Ahmad. 2021. Investigation of soil erosion in Pothohar Plateau of Pakistan. Pak. J. Agric. Res., 34(2): 362-371. https://doi.org/10.17582/journal.pjar/2021/34.2.362.371

Tsegaye, L., and R. Bharti. 2021. Soil erosion and sediment yield assessment using RUSLE and GIS-based approach in Anjeb watershed, Northwest Ethiopia. SN Appl. Sci., 3(5): 1–19. https://doi.org/10.1007/s42452-021-04564-x

Ullah, S., N.M. Syed, T. Gang, R.S. Noor, S. Ahmad, M.M. Waqas and S. Ullah. 2022. Recent global warming as a proximate cause of deforestation and forest degradation in northern Pakistan. PLoS One, 17(1): 3–4. https://doi.org/10.1371/journal.pone.0260607

Ullah, S., A. Ali, M. Iqbal, M. Javid and M. Imran. 2018. Geospatial assessment of soil erosion intensity and sediment yield: A case study of Potohar Region, Pakistan. Environ. Earth Sci., 77(19): 1–13. https://doi.org/10.1007/s12665-018-7867-7

Walling, D.E., 2011. Human impact on the sediment loads of Asian rivers. IAHS-AISH Publication, 349(3): 37–51.

Wang, J., P. Lu, D. Valente, I. Petrosillo, S. Babu, S. Xu and M. Liu. 2022. Analysis of soil erosion characteristics in small watershed of the loess tableland Plateau of China. Ecol. Ind., 137(1): 108765. https://doi.org/10.1016/j.ecolind.2022.108765

Wiejaczka, L., J.R. Olędzki, A. Bucała-Hrabia and M. Kijowska-Strugała. 2017. A spatial and temporal analysis of land use changes in two mountain valleys: With and without dam reservoir (Polish Carpathians). Quaest. Geogr., 36(1): 129–137. https://doi.org/10.1515/quageo-2017-0010

Wischmeier, W.H., and D.D. Smith. 1978. Predicting rainfall erosion losses, a guide to conservation planning. Predicting Rainfall Erosion Losses. A Guide Conserv. Plann.,

Wuepper, D., P. Borrelli and R. Finger. 2020. Countries and the global rate of soil erosion. Nat. Sustain., 3(1): 51–55. https://doi.org/10.1038/s41893-019-0438-4

Yang, D., S. Kanae, T. Oki, T. Koike and K. Musiake. 2003. Global potential soil erosion with reference to land use and climate changes. Hydrol. Process., 17(14): 2913–2928. https://doi.org/10.1002/hyp.1441

Yesuph, A.Y., and A.B. Dagnew. 2019. Soil erosion mapping and severity analysis based on RUSLE model and local perception in the Beshillo Catchment of the Blue Nile Basin, Ethiopia. Environa. Syst. Res., 8(1): 1–21. https://doi.org/10.1186/s40068-019-0145-1

Zamani, A., A. Sharifi, S. Felegari, A. Tariq and N. Zhao. 2022. Agro climatic zoning of saffron culture in miyaneh city by using WLC method and remote sensing data. Agriculture (Switzerland), 12(1): 1–15. https://doi.org/10.3390/agriculture12010118